Original Article

64-multidetector CT anatomical assessment of the feline bronchial and pulmonary vascular structures

Ioannis Panopoulos[1] iD, Edoardo Auriemma[2], Swan Specchi[2], Alessia Diana[3], Marco Pietra[3], Anastasia Papastefanou[4], Eric Zini[5,6,7] and Mario Cipone[3]

Abstract

Objectives The aim of the study was to provide a detailed anatomical study of the feline bronchial and vascular structures by using CT angiography (CTA).

Methods Adult cats with no respiratory clinical signs were enrolled in a CTA protocol to provide an anatomical study of the thorax. The dimensions, number of branches and branching pattern (monopodial vs dichotomic) of both bronchial and pulmonary vascular structures were evaluated under positive inspiration apnoea. A linear generalised estimating equations analysis (Spearman's rho) was used to identify statistical correlation between tracheal diameter, age and body weight of the cats.

Results Fourteen cats met the inclusion criteria. The pulmonary arteries had larger diameters than the pulmonary veins, and the pulmonary veins had larger diameters than the bronchial structures. A higher number of segmental bronchial and pulmonary vascular branches was observed in the left caudal lung lobe than in the other lobes. The monopodial branching pattern of both bronchial and pulmonary vascular structures was predominant in all cats of our study (100%) in cranial, caudal and right middle lung lobes, while a dichotomic branching pattern of the bronchial and pulmonary vascular structures of the accessory lung lobe was seen in 13 cats (93%). Thirteen cats (93%) had three pulmonary vein ostia, and one cat (7%) also presented with an additional left intermediate pulmonary vein ostium. Variation in the number of segmental pulmonary vein branches was noted in the right caudal lung lobe. There was no statistical correlation between tracheal diameter, age and weight.

Conclusions and relevance Architecture of the feline bronchovascularr structures belongs to a mixed type of monopodial and dichotomic branching pattern. In cats, the pulmonary venous drainage system predominately presents three pulmonary vein ostia. Variations in the type of formation and the number of branches of the pulmonary venous drainage system were noted.

Keywords: Computed tomography; angiography; thorax; pulmonary vessels

[1]Department of Diagnostic Imaging, Alphavet, Kifisia, Athens, Greece
[2]Department of Diagnostic Imaging, Veterinary Institute of Novara, Novara, Italy
[3]Department of Veterinary Medical Sciences, University of Bologna, Italy
[4]Department of Anesthesiology, Optivet Referrals, Hampshire, UK
[5]Clinic for Small Animal Internal Medicine, Zurich University, Vetsuisse-Faculty, Zurich, Switzerland
[6]Department of Animal Medicine, Production and Health, University of Padua, Legnaro, Italy
[7]Department of Internal Medicine, Istituto Veterinario di Novara, Novara, Italy

Corresponding author:
Ioannis Panopoulos DVM, PhD, Veterinary Institute of Novara, Strada Provinciale 9, Granozzo con Monticello, 28100 Novara, Italy
Email: ioannis.panopoulos.vetrad@gmail.com

Introduction

Multi-detector CT (MDCT) has become a routine examination tool, and the utility and accuracy of it as an advanced imaging diagnostic tool for the screening of feline thoracic pathologies has been demonstrated.[1–10] A CT comparison of the normal cross-sectional anatomy of the feline thorax has previously been described.[11] More recently, several reports described threshold values for pulmonary artery and bronchial lumen diameters in cats with and without cardiopulmonary pathologies in order to define imaging criteria useful to diagnose feline bronchiectasis.[12–14] Bronchial wall thickness was also evaluated in healthy and asthmatic cats to correlate this parameter with feline asthma.[15] Nevertheless, to the best of our knowledge, there is a lack of information in the literature regarding detailed imaging and gross anatomy of the feline bronchial tree, pulmonary arteries, pulmonary veins and pulmonary venous ostia.

The aim of this study was to provide an anatomical description of the bronchial tree, pulmonary arteries and pulmonary veins by using 64-MDCT angiography.

Materials and methods

This was a prospective descriptive anatomical study. Informed owner consent was obtained, and the ethical committee of the University of Bologna approved the protocol of the study. Twenty cats with normal clinical examination, normal complete blood test and urine analysis, negative faecal examination, normal thoracic CT and no history of respiratory disease were included. Exclusion criteria included CT findings compatible with thoracic and pulmonary disease. The study was performed with a 64-MDCT scanner (Toshiba Aquilion 64). After pre-anaesthetic assessment, each cat received 25 μg/kg of dexmedetomidine and 0.1 mg/kg of butorphanol IM. The cats were induced to general anaesthesia with 1–2 mg/kg of propofol IV to effect and intubated via an endotracheal tube. General anaesthesia was maintained with isoflurane in 100% oxygen through a Bain breathing system, with an oxygen flow rate of 2 l/min. Normocapnia was maintained with intermittent positive pressure ventilation whenever necessary.

Cats were positioned in sternal recumbency with the limbs extended forwards. Pre- and post-contrast series of the thorax were performed during inspiratory apnoea (peak inspiration pressure maintained at 15 cm H_2O) by using 0.5 mm slice thickness, 0.5 second tube rotation time, 120 kVp and 50 mA, scanning from the thoracic inlet to the cranial abdomen. An intravenous saline flush of 3 ml/kg with a rate of injection 2 ml/s was performed twice, once before the injection of contrast medium and once immediately afterwards. Iodinated non-ionic contrast medium (Iobitridol, 300 mgI/ml) was injected via a dual-barrel injector system with a heating cuff, extravasation detection device and communication interface between the scanner

Table 1 Abbreviations of the bronchial structures

Abbreviations	Bronchial structures
RPB	Right principal bronchus
RB1	Right cranial lobe
RB1D1	Dorsolateral branch of the right cranial lobe
RB1V1	Ventral branch of the right cranial lobe
RB2	Middle lobe
RB2R1	Cranial branch of the middle lobe
RB2C1	Caudal branch of the middle lobe
RB3	Accessory lobe
RB3V1	Ventromedial branch of the accessory lobe
RB3D1	Caudal branch of the accessory lobe
RB4	Right caudal lobe
RB4V1	Ventral branch of the right caudal lobe
RB4V2	Caudoventral branch of the right caudal lobe
RB4V3	Caudal branch of the right caudal lobe
LPB	Left principal bronchus
LB1	Left cranial lobe
LB1D1	Cranioventral branch of the left cranial lobe
LB1V1	Caudoventral branch of the left cranial lobe
LB2	Left caudal lobe
LB2V1	Ventral branch
LB2V2	Caudoventral branch of the left caudal lobe
LB2V3	Caudal branch of the left caudal lobe

and the injector. Contrast medium was kept at 37°C within the dual/barrel injector system and injected with a constant rate of 2 ml/s, with a total dose of 600 mgI/kg and maximum pressure of 300 lb/in².

To determine the starting delay of the post-contrast series, the time to peak enhancement was set by using a bolus tracking technique. The region of interest was drawn within the descending aorta at the level of the eighth thoracic vertebra, arbitrarily choosing a descending aorta opacification threshold of 115 Hounsfield units above baseline (Sure Start proprietary software; Toshiba Medical Systems) for starting the post-contrast thoracic scan. Images were reconstructed with soft tissue and lung algorithms and the acquired data were exported to a dedicated workstation (Vitrea; Vital Images) for post-processing elaboration of the data. Multiplanar reformatted reconstruction surface rendering, maximum intensity projection, volume rendering and endoluminal segmentation were used to evaluate the pulmonary vasculature and bronchial anatomical structures. Each segment of the bronchial tree was named according to the endoscopic classification system as previously described (Table 1).[16]

All images were reviewed by two investigators (IP and MC) and the following parameters were assessed. (1) Number and diameter of the tracheobronchial segments and pulmonary arteries and veins and their anatomical correlation in the thoracic cavity. The diameter
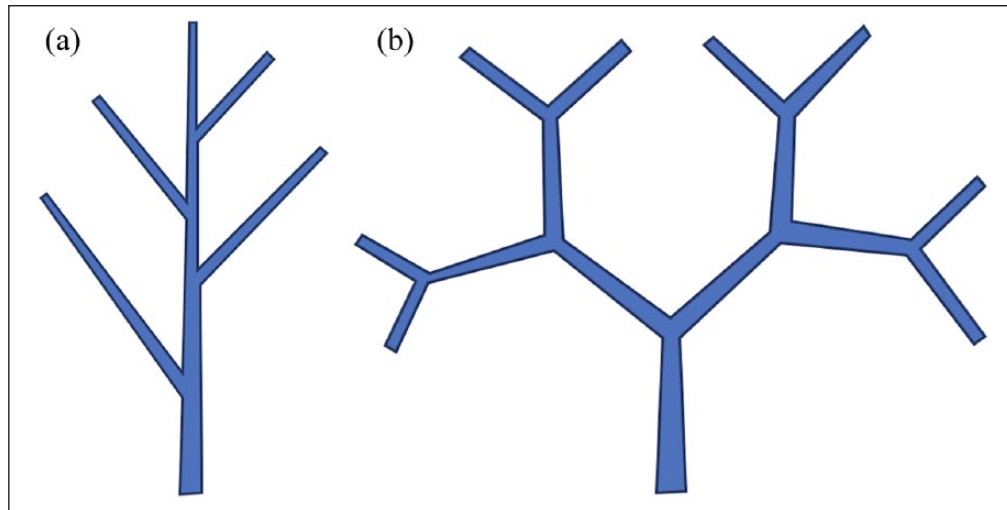
Figure 1 (a) Monopodial branching pattern and (b) dichotomic branching pattern

of the tracheobronchial tree and vascular segments was calculated by applying calipers from inner to inner edge (referring to the luminal diameter avoiding the parietal wall thickness), with a constant window level of –340 and window width of 1700. Each segment was measured four times in three planes (ie, twice in transverse, once in sagittal and once in coronal planes). The tracheal diameter was measured immediately proximal to the bifurcation and each lobar and segmental bronchial or vascular branch was measured just distal to its origin. The anatomical position of each pulmonary artery and vein was evaluated relative to their corresponding bronchi.

(2) Monopodial or dichotomic patterns of distribution of the bronchial and vascular structures. In the monopodial distribution, the main central bronchial or vascular segment branches off in multiple smaller segments, whereas in the dichotomic distribution the main central segment bifurcates into two branches of equal diameters and from each of these are multiple smaller branches (Figure 1).

(3) Number of the pulmonary vein ostia within the left atrium and classification of the pulmonary venous drainage system just before the opening in the pulmonary vein ostia (ie, separate, short common trunk and long common trunk; as seen in Figure 2). The pulmonary venous drainage system was classified as: (a) separate, when the pulmonary veins drained independently in the left atrium; (b) short common trunk, when two or more pulmonary veins fused by forming a 'short neck' just before opening into the left atrium; or (c) long common trunk, when two or more pulmonary veins fused by forming a 'long neck' just before opening into the left atrium

Statistical analysis
A Spearman's rho analysis was used to identify statistical correlation between tracheal diameter and age or body weight of our group of cats. Analyses were achieved with commercial software (IBM SPSS Statistics, release 22.0.0.0, 64-bit edition). $P < 0.05$ was considered statistically significant.

Results
Six cats were excluded from the study owing to detection of pulmonary lesions (five cats) and mild spontaneous pneumothorax (one cat). Fourteen domestic shorthair cats (nine males and five females) met the inclusion criteria with a median age of 1.7 years (range 1–6 years) and median body weight of 4.3 kg (range 2.7–6.7 kg).

Number and diameter of bronchovascular segments
The tracheobronchial tree ramification was consistent in all 14 cats. The trachea bifurcated into the right and left main bronchi. The right main bronchus branched off into the right cranial, middle, accessory and caudal secondary bronchi, and the left main bronchus further divided into the left cranial and caudal secondary bronchi.

The right cranial bronchus (RB1) ran cranioventrally, bifurcating into two main dorsolateral and ventral branches and further into multiple segmental smaller bronchi. The pulmonary arteries and pulmonary veins ran dorsolaterally and ventromedially, respectively, to the corresponding bronchial structures. The pulmonary veins of the right cranial lobe merged before receiving the drainage of the pulmonary vein of the middle lung lobe.

The right middle bronchus (RB2) originated directly from the right main bronchus just caudal to the origin of the RB1, ran caudoventrally close to the cardiac surface and further divided into multiple cranioventral and caudoventral branches. The pulmonary arteries and
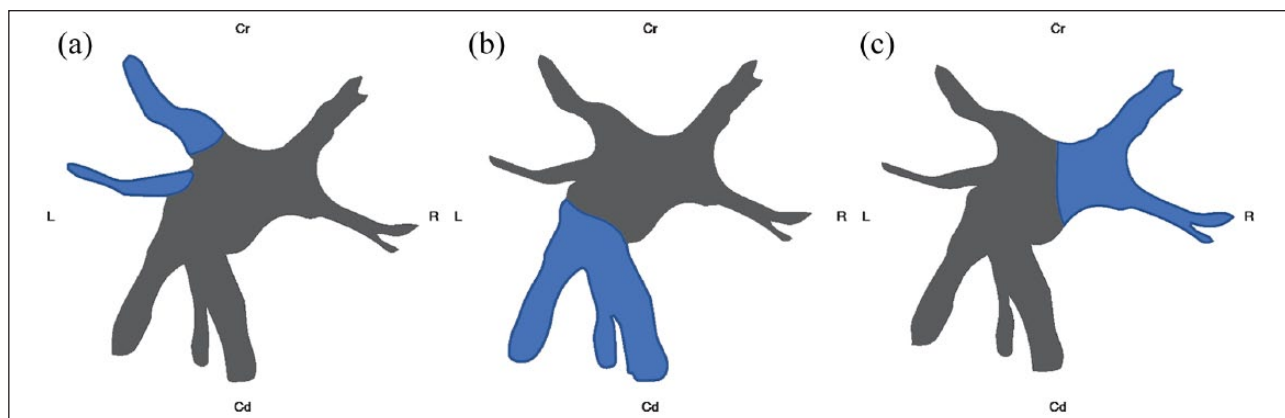
Figure 2 Classification of the pulmonary venous drainage system as (a) separate, (b) short common trunk and (c) long common trunk. Cr = cranial; Cd = caudal; L = left; R = right

veins of the right middle lobe ran laterally and medially, respectively, to the corresponding bronchial branches.

The accessory bronchus (RB3) originated from the medial wall of the right caudal bronchus at the level of its origin, ran caudoventromedially and bifurcated into ventromedial and caudal branches such as its corresponding pulmonary arterial and venous branches. The pulmonary arteries and veins of the accessory lung lobe ran ventrally and dorsally, respectively, to the corresponding bronchial branches. The pulmonary veins of the accessory lobe merged before joining the right caudal pulmonary vein.

The right caudal bronchus (RB4) branched off as a direct continuation of the right main bronchus, just caudal to the origin of the RB3. The RB4 had three main segmental bronchial branches (ventral, caudoventral and caudal) followed by corresponding pulmonary arteries and veins (Figure 3a). In eight (57%) cats (six males, two females), we noted the absence of the caudoventral pulmonary vein; this area was drained by the adjacent ventral and caudal branches of the pulmonary vein of the right caudal lobe (Figure 3b). The pulmonary arteries and pulmonary veins ran dorsolaterally and ventromedially, respectively, to the corresponding bronchial structures.

The left main bronchus branched off immediately after the tracheal bifurcation laterally the left cranial (LB1) and caudally the left caudal (LB2) lobar bronchi.

The LB1 further split into two rami, one running cranioventrally and one caudoventrally, leading to multiple segmental dorsal and ventral branches. The pulmonary arteries and pulmonary veins ran dorsolaterally and ventromedially, respectively, to the corresponding bronchial structures.

The LB2 originated as a direct continuation of the left main bronchus, just caudal to the origin of the LB1. The LB2 branched into three main rami (ventral, caudoventral and caudal). The pulmonary arteries and veins of the LB2 branched off according to the bronchial ramifications. The pulmonary arteries and pulmonary

veins ran dorsolaterally and ventromedially, respectively, to the corresponding bronchial structures.

The mean diameters of the bronchial and vascular structures are summarised (Table 2).

The pulmonary arteries had a larger diameter than the corresponding pulmonary veins and the pulmonary veins had a larger diameter than the corresponding bronchial segments. A higher number of segmental
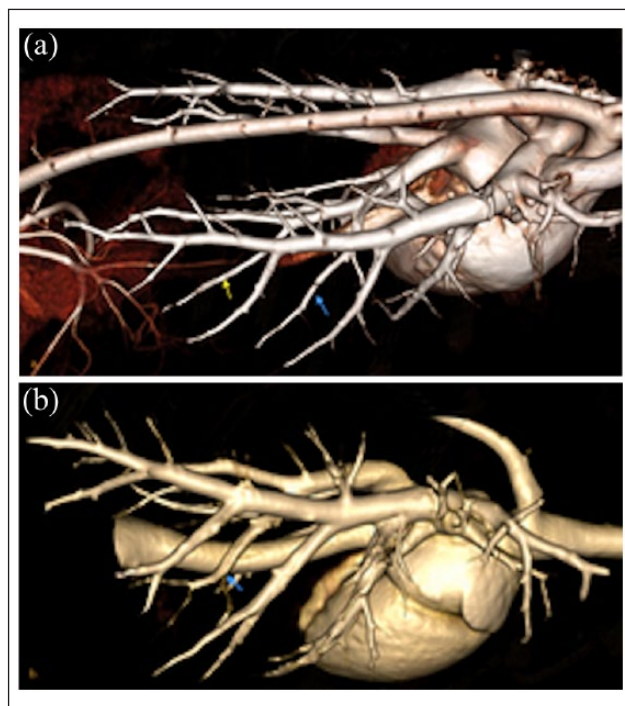

Figure 3 (a) The right caudal pulmonary vein had both the ventral (blue arrow) and caudoventral pulmonary vein (yellow arrow. (b) The caudoventral pulmonary vein does not exist; the area was drained by the ventral (blue arrow) and caudal pulmonary vein branches of the right caudal lobe

Table 2 Mean diameter of the bronchovascular structures

Segments	Mean bronchial diameter (mm)	Mean pulmonary arterial diameter (mm)	Mean pulmonary vein diameter (mm)
RB1	3.77	4.73	3.93
RB1D1	1.63	2.03	1.96
RB1V1	3.15	3.35	2.7
RB2	2.21	2.78	2.31
RB2R1	1.05	1.31	1.03
RB2C1	1.54	2.22	1.69
RB3	2.12	2.8	2.41
RB3V1	1.53	1.93	1.72
RB3D1	1.33	1.87	1.37
RB4	3.9	4.78	3.99
RB4V1	1.75	2.51	2.44
RB4V2	1.71	2.19	1.49
RB4V3	2.82	3.35	2.45
LB1	3.21	5.49	3.21
LB1D1	2.24	3.21	2.49
LB1V1	1.94	2.86	2.38
LB2	3.83	5.02	4.39
LB2V1	1.81	2.32	2.25
LB2V2	1.76	2.18	1.72
LB2V3	3.02	3.36	2.38

See Table 1 for a description of the abbreviations

bronchovascular branches was observed in the left caudal lung lobe than in the remaining lung lobes (Table 3).

Monopodial or dichotomic pattern of distribution of the bronchial and vascular structures

The type of distribution pattern of the bronchial tree is summarised in Table 4. In our study, most of the bronchovascular segments matched a monopodial classification.

More specifically, in all 14 cats of our study, both bronchial and pulmonary vascular structures of the cranial and caudal and the middle lung lobes had a monopodial branching pattern. In 13 cats both bronchial and pulmonary vascular structures of the accessory lobe had a dichotomic branching pattern, while just one cat had a monopodial branching pattern.

Number of pulmonary vein ostia within the left atrium and classification of pulmonary venous drainage system

The pulmonary veins drained into the left atrium via three ostia (right cranial, left cranial and caudodorsal) in all cats in our study (Figure 4).

The right cranial ostium (RO) received the drainage of the right cranial and middle lung lobes. The right

Table 3 Mean number of segmental pulmonary branches

LB1D1-dor	LB1D1-ve	LB1V1-cr	LB1V1-cd	LB2-dor	LB2-ve	RB1D1-dor	RB1D1-ve	RB1V1-dor	RB1V1-ve	RB2-cr	RB2-cd	RB3D1-dor	RB3D1-ve	RB3V1-cr	RB3V1-cd	RB4-dor	RB4-ve
10.64	9.14	4.29	8.57	13.5	11.36	1	1	9.14	8.07	6.5	7.64	5.57	5.36	3.64	3.57	11.46	9.21

dor = dorsal; ve = ventral; cr = cranial; cd = caudal; see Table 1 for a description of the remaining abbreviations

Table 4 Branching patterns of the bronchial and vascular segments

Branching pattern	RB1	RB2	RB3	RB4	LB1	LB2
Monopodial	14	14	1	14	14	14
Dichotomic	0	0	13	0	0	0

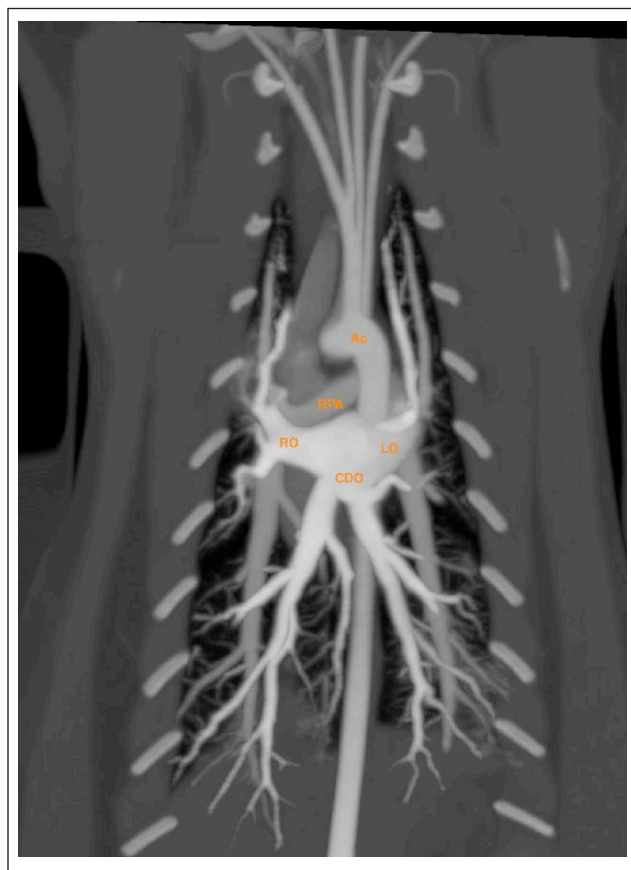See Table 1 for a description of the abbreviations

Figure 4 Maximum intensity projection reconstruction of the pulmonary vasculature in coronal plane. Ao = aorta; RPA = right pulmonary artery; LO = left cranial ostium; CDO = caudodorsal ostium; RO = right cranial ostium

cranial lobar pulmonary vein merged with the right middle lobar pulmonary vein by forming a long common trunk before opening into the right cranial part of the left atrium (ie, the RO) in all cats (100%) of our study.

The left cranial ostium (LO) hosted the drainage of the lobar pulmonary veins of the cranial and caudal portions of the left cranial lung lobe, which joined together via a long common trunk before opening into the left cranial part of the left atrium (ie, LO). The long common trunk type of venous drainage between the left cranial lobar veins was noted in 13 cats (93%), whereas in one cat (7%) the lobar pulmonary veins of the cranial and

caudal portion of the left cranial lung lobe opened up separately and into the left atrium via the LO and an intermediate adjacent ostium, respectively (Figure 5).

The caudodorsal ostium (CDO) received the drainage of both the caudal and accessory lobar pulmonary veins. In all cats (100%) the right caudal lobar pulmonary vein received the accessory lobar pulmonary vein and fused with the left caudal lobar pulmonary vein by forming a short common venous trunk that opened into the caudodorsal part of the left atrium (ie, CDO).

There was no statistical correlation between the tracheal diameter, age and body weight of our group of cats.

Discussion

We successfully depicted feline bronchovascular structures by using a 64-MDCT in 14 cats. In all cats, the trachea bifurcated into right and left main bronchi, consistent with the current literature and similar to canine anatomy.[16–20] No statistical correlation was observed between tracheal diameter, age and body weight; we deemed this logical owing to the fact that our population included adult cats (>1 year old) in which complete physical growth and maturation was expected.

As described in earlier feline literature, we noted that the pulmonary arteries had a larger diameter than the corresponding bronchi.[12,13,15] However, in normal dogs the bronchi tend to have a larger diameter than the adjacent pulmonary arteries, with a bronchial lumen to pulmonary artery ratio range of 0.8–2.0.[21,22] Based on previous literature, a peak inspiration pressure of 15 cm H_2O was chosen in order to avoid motion artefacts during image acquisition.[7,8,12–14,23,24] Pulmonary arteries predominantly ran dorsolaterally to the corresponding bronchus, whereas pulmonary veins ran ventromedially to the corresponding bronchus. An exception was seen in the accessory lung lobe, where the pulmonary arteries ran ventrally and the pulmonary veins ran dorsally to their corresponding bronchus.

To the best of our knowledge, no imaging studies have previously correlated the diameter of the feline pulmonary arteries with the corresponding pulmonary veins. Of all the cats in our study we consistently noted that the pulmonary veins had a smaller diameter than the corresponding arteries; this finding is in agreement with available medical literature.[25,26] The pulmonary vein to pulmonary artery ratio has been recently
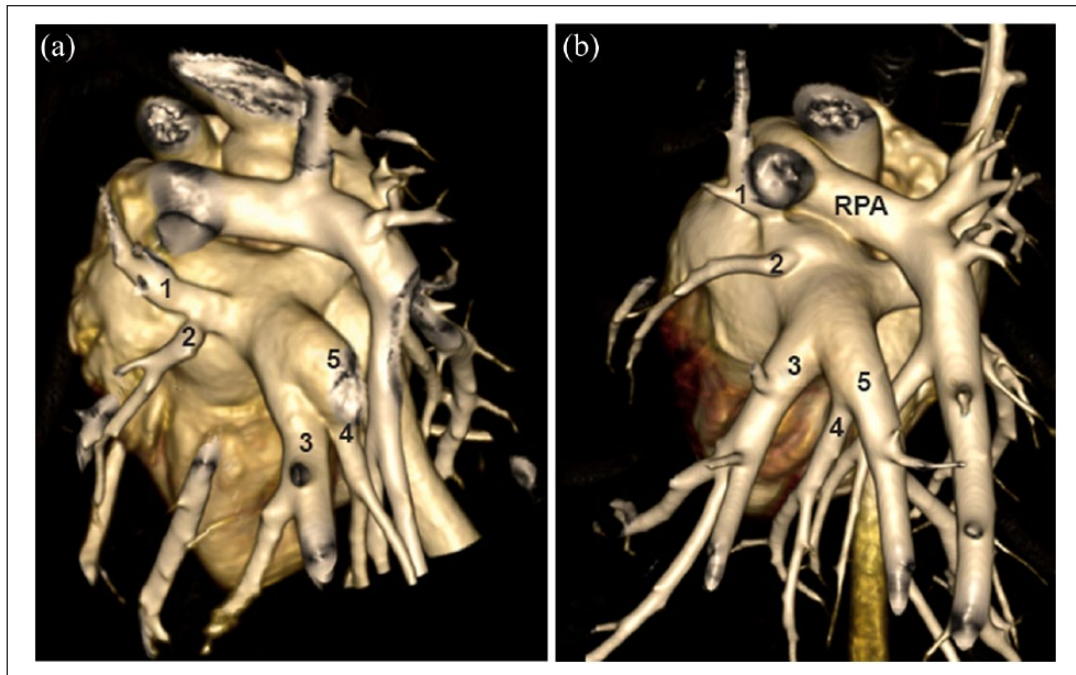
Figure 5 Two different aspects of the left cranial ostium: (a) the cranioventral branch of the pulmonary vein of the left cranial lobe (LB1D1) and the caudoventral branch of the pulmonary vein of the left cranial lobe (LB1V1) anastomose before draining the left atrium; (b) the LB1D1 and the LB1V1 drain into the left atrium separately. 1 = LB1D1; 2 = LB1V1; 3 = left caudal lobe pulmonary vein; 4 = accessory lobe pulmonary vein; 5 = right caudal pulmonary vein; RPA = right pulmonary artery

proposed in dogs as an echocardiographic index to identify early left-sided congestive heart failure.[27,28] Further studies correlating the diameter of pulmonary veins and arteries in cats affected by left-sided congestive heart failure are needed in order to understand if such an index could also be a useful diagnostic tool in the feline population.

According to the literature, the monopodial lobar bronchovascular branching pattern is predominant in dogs, while the human bronchial tree is consistent with a dichotomic classification.[29–31] No monopodial or dichotomic classification has been proposed for the feline population. Based on our results, the feline bronchial and pulmonary vascular structures demonstrated a predominant lobar monopodial architecture with the exception of the accessory lobe, which demonstrated a prevalent dichotomic branching pattern. The dichotomic or monopodial bronchial branching patterns may influence the distribution of gas.[29,30] In dogs, it is believed that, owing to the monopodial branching pattern, there is a preferential distribution of ventilation to peripheral regions of the lung, which is more pronounced during higher inspiratory flow rates.[30] Further studies are needed to investigate the possible correlation between the predominant feline monopodial bronchial branching pattern and preferential peripheral lung ventilation.

Pulmonary variations of the venous system are well studied in humans as pulmonary veins are an important source of ectopic atrial electrical activity, frequently initiating paroxysms of atrial fibrillation.[32] In humans, four pulmonary vein ostia are usually present with variable distribution, and variations in pulmonary vein drainage systems have been correlated with arrhythmia or, in one case, high altitude pulmonary oedema.[33–35] In our study the left-sided venous drainage system is more variable than the right one; this differs from humans, in which there is more variability in the right-sided venous drainage system.[36] Canine anatomical variations of the pulmonary and cardiac venous system are poorly reported.[37,38] The porcine and equine models of the pulmonary venous system are documented to be similar to humans and they present neuron cell bodies at the venoatrial junction and alongside the myocardial sleeve. These neuron cell bodies could play an important role in the induction of atrial fibrillation, a fact that has not been documented in the feline population until now. In horses, a larger ostium usually demonstrates a longer myocardial sleeve. Further studies measuring the volume of the feline ostium in correlation with the length of the pulmonary venous trunk/myocardial sleeve are needed to identify possible similar findings in the feline population.[39,40]

To our knowledge, this is the first report that attempted to classify the pulmonary venous drainage and corresponding pulmonary vein ostia in cats. The long common trunk venous drainage was the predominant type of pulmonary vein anastomosis seen in our case series before emptying within the left and right cranial pulmonary vein ostia; a vascular variation was detected in only one cat in which an additional intermediate ostium was detected between the left cranial and the caudodorsal ostia. The short common trunk venous drainage was the only type of pulmonary vein anastomosis of the caudodorsal pulmonary vein ostium.

Feline cardiogenic pulmonary oedema is well documented and shows extreme variability in its radiographic distribution compared with canine species; to date, there is no clear explanation of the variable presentation of the feline cardiogenic pulmonary oedema.[41–43] Further studies are needed to identify possible correlation between pulmonary venous drainage variation in the left atrium and manifestation of feline cardiovascular imbalances.

The limited number of cats and the absence of gross anatomy were the two main limitations of our study. A third limitation was the absence of a complete cardiological and echocardiographic examination, not allowing us to exclude any underlying subclinical cardiac disease. Another limitation was the absence of a comparison study using different peak inspiration pressures or spontaneous respiration during the acquisition of the images, aimed at evaluating the effect on the diameter of the bronchovascular structures. To date, no data have been reported in the feline literature correlating the influence of the anaesthetic protocol and the pressure used during the positive inspiration apnoea with the dimensions of the feline bronchial and vascular structures. Considering that the bronchial structures in our study had smaller diameters than vascular structures, we hypothesise that performing a positive ventilation anaesthetic protocol with lower peak pressure, simulating normal respiratory conditions, could lead to a smaller bronchial diameter.

Conclusions

Thoracic CT angiography in cats under positive ventilation showed that pulmonary arteries had larger diameters than the pulmonary veins, while the pulmonary veins had larger diameters than the corresponding bronchi. The feline bronchovascular branching pattern is predominantly monopodial. There was no statistical correlation between the tracheal diameter, age and body weight of our group of cats. In all cats in the study the pulmonary veins fused by forming three pulmonary vein ostia and formed a long common trunk in the left and right cranial pulmonary vein ostia, and a short common trunk in the caudodorsal pulmonary vein ostium.

ORCID iD Ioannis Panopoulos (iD) https://orcid.org/0000-0001-8496-2159

References

1 Byrne P, Berman JS, Allan GS, et al. **CT findings in two cats with broncholithiasis**. *JFMS Open Rep* 2016; 15. DOI: 10.1177/2055116916676176.

2 Lacava G, Zini E, Marchesotti F, et al. **Computed tomography, radiology and echocardiography in cats naturally infected with *Aelurostrongylus abstrusus***. *J Feline Med Surg* 2017; 19: 446–453.

3 Major A, Holmes A, Warren-smith C, et al. **Computed tomographic findings in cats with mycobacterial infection**. *J Feline Med Surg* 2016; 18: 510–517.

4 Aarsvold S, Reetz JK, Reichle JK, et al. **Computed tomographic findings in 57 cats with primary pulmonary neoplasia**. *Vet Radiol Ultrasound* 2015; 56: 272–277.

5 Dillon AR, Tillson DM, Wooldridge A, et al. **Effect of precardiac and adult stages of *Dirofilaria* immitis in pulmonary disease of cats: CBC, bronchial lavage cytology, serology, radiographs, CT images, bronchial reactivity and histopathology**. *Vet Parasitol* 2014; 206: 24–37.

6 Trzil JE, Masseau I, Webb TL, et al. **Long-term evaluation of mesenchymal stem cell therapy in a feline model of chronic allergic asthma**. *Clin Exp Allergy* 2014; 44: 1546–1557.

7 Dennler M, Bass DA, Gutierrez-Crespo B, et al. **Thoracic computed tomography, angiographic computed tomography and pathology findings in six cats experimentally infected with *Aelurostrongylus abstrusus***. *Vet Radiol Ultrasound* 2013; 54: 459–469.

8 Dillon AR, Tillson DM, Hathcock J, et al. **Lung histopathology, radiography, high-resolution computed tomography, and bronchio-alveolar lavage cytology are altered by *Toxocara cati* infection in cats and is independent of development of adult intestinal parasites**. *Vet Parasitol* 2013; 193: 413–426.

9 Henninger W. **Use of computed tomography in the diseased feline thorax**. *J Small Anim Pract* 2003; 44: 56–64.

10 Hahn H, Specchi S, Masseau I, et al. **The computed tomographic "tree-in-bud" pattern: characterization and comparison with radiographic and clinical findings in 36 cats**. *Vet Radiol Ultrasound* 2017; 59: 32–42.

11 Samii VF, Biller DS and Koblik P. **Normal cross-sectional anatomy of the feline thorax and abdomen: comparison of computed tomography and cadaver anatomy**. *Vet Radiol Ultrasound* 1998; 39: 504–511.

12 Reid LE, Dillon AR, Hathcock JT, et al. **High-resolution computed tomography bronchial lumen to pulmonary artery diameter ratio in anesthetized ventilated cats with normal lungs**. *Vet Radiol Ultrasound* 2012; 53: 34–37.

13 Lee-Fowler TM, Cole RC, Dillon AR, et al. **High-resolution computed tomography evaluation of the bronchial lumen to vertebral body diameter and pulmonary artery to vertebral body diameter ratios in anesthetized ventilated normal cats**. *J Feline Med Surg* 2017; 19: 1007–1012.

14 Lee-Fowler TM, Cole RC, Dillon AR, et al. **High-resolution CT evaluation of bronchial lumen to vertebral body, pulmonary artery to vertebral body and bronchial lumen to pulmonary artery ratios in *Dirofilaria immitis*-infected cats with and without selamectin administration**. *J Feline Med Surg* 2018; 20: 928–933.

15 Won S, Yun S, Lee J, et al. **High resolution computed tomographic evaluation of bronchial wall thickness in healthy and clinically asthmatic cats**. *J Vet Med Sci* 2017; 79: 567–571.

16 Caccamo R, Twedt DC, Buracco P, et al. **Endoscopic bronchial anatomy in the cat**. *J Feline Med Surg* 2007; 9: 140–149.

17 Barone R. Anatomia comparata dei mammiferi domestici. vol iii: splancnologia – apparecchio digerente e respiratorio. Bologna: Ed Agricole, 2003.

18 Getty R. Anatomia degli animali domestici. Volume II. Padova: Piccin Editore, 1982.

19 Ishaq M. **A morphological study of the lungs and bronchial tree of the dog: with a suggested system of nomenclature for bronchi**. *J Anat* 1980; 131: 589–610.

20 Evan He and de Lahunta A (eds). Miller's anatomy of the dog. 4th ed. St Louis, MO: Elsevier, 2013.

21 Cannon MS, Wisner ER, Johnson LR, et al. **Computed tomography bronchial lumen to pulmonary artery diameter ratio in dogs without clinical pulmonary disease**. *Vet Radiol Ultrasound* 2009; 50: 622–624.

22 Horsfield K, Kemp W and Phillips S. **Diameters of arteries, veins, and airways in isolated dog lung**. *Anat Rec* 1986; 216: 392–395.

23 Henao-Guerrero N, Ricco C, Jones J, et al. **Comparison of four ventilatory protocols for computed tomography of the thorax in healthy cats**. *Am J Vet Res* 2016; 73: 646–653.

24 Guarracino A, Lacitignola L, Auriemma E, et al. **Which airway pressure should be applied during breath-hold in dogs undergoing thoracic computed tomography?** *Vet Radiol Ultrasound* 2016; 57: 475–481.

25 Kim YH, Marom EM, Herndon JE 2nd, et al. **Pulmonary vein diameter, cross-sectional area, and shape: CT analysis**. *Radiology* 2005; 235: 43–49.

26 Bozlar U, Ors F, Deniz O, et al. **Pulmonary artery diameters measured by multidetector-row computed tomography in healthy adults**. *Acta Radiol* 2007; 48: 1086–1091.

27 Merveille AC, Bolen G, Krafft E, et al. **Pulmonary vein-to-pulmonary artery ratio is an echocardiographic index of congestive heart failure in dogs with degenerative mitral valve disease**. *J Vet Intern Med* 2015; 29: 1502–1509.

28 Birettoni F, Caivano D, Patata V, et al. **Canine pulmonary vein-to-pulmonary artery ratio: echocardiographic technique and reference intervals**. *J Vet Cardiol* 2016; 18: 326–335.

29 Schlesinger RB and McFadden LA. **Comparative morphometry of the upper bronchial tree in six mammalian species**. *Anat Rec* 1981; 199: 99–108.

30 Wang PM and Kraman SS. **Fractal branching pattern of the monopodial canine airway**. *J Appl Physiol* 2004; 96: 2194–2199.

31 Monteiro A and Smith RL. **Bronchial tree architecture in mammals of diverse body mass**. *Int J Morphol* 2014; 32: 312–316.

32 Marom E, Herndon J, Kim Y, et al. **Variations in pulmonary venous drainage to the left atrium: implications for radiofrequency ablation**. *Radiology* 2004; 230: 824–829.

33 Tekbas G, Gumus H, Onder H, et al. **Evaluation of pulmonary vein variations and anomalies with 64 slice multi detector computed tomography**. *Wien Klin Wochenschr* 2012; 124: 3–10.

34 Harbi A, Mhish H, Alshehri HZM, et al. **Anatomical variation of pulmonary venous ostium and its relationship with atrial arrythmia in the Saudi population**. *J Saudi Heart Assoc* 2014; 26: 81–85.

35 Derks A and Bosch FH. **High-altitude pulmonary edema in partial anomalous pulmonary venous connection of drainage with intact atrial septum**. *Chest* 1991; 103: 973–974.

36 Wannasopha Y, Oilmungmool N and Euathongchit J. **Anatomical variations of pulmonary venous drainage in Thai people: multidetector CT study**. *Biomed Imaging Interv J Open Rep* 2012; 8. DOI: 10.2349/biij.8.1.e4.

37 Brewer FC, Moise NS, Kornreich BG, et al. **Use of computed tomography and silicon endocasts to identify pulmonary veins with echocardiography**. *J Vet Cardiol* 2012; 14: 293–300.

38 Abraham LA and Slocombe RF. **Asymptomatic anomalous pulmonary veins in a Siberian husky**. *Aust Vet J* 2003; 81: 406–408.

39 Vandecasteele T, Cornillie P, Van Steenkiste G, et al. **Echocardiographic identification of atrial-related structures and vessels in horses valitated by computed tomography of casted hearts**. *Equine Vet J*. Epub ahead of print 28 May 2018. DOI: 10.1111/evj.12969.

40 Vandecasteele T, Van Den Broeck W, Tay H, et al. **3D reconstruction of the porcine and equine pulmonary veins, supplemented with the identification of telocytes in the horse**. *Anat Histol Embryol* 2018; 47: 145–152.

41 Guglielmini C and Diana A. **Thoracic radiography in the cat: identification of cardiomegaly and congestive heart failure**. *J Vet Cardiol* 2015; 17 Suppl 1: S87–S101.

42 Benigni L, Morgan N and Lamb CR. **Radiographic appearance of cardiogenic pulmonary oedema in 23 cats**. *J Small Anim Pract* 2009; 50: 9–14.

43 Schober Ke, Wetli E and Drost WT. **Radiographic and echocardiographic assessment of the left atrial size in 100 cats with acute left-sided congestive heart failure**. *Vet Radiol Ultrasound* 2014; 55: 359–367.